General Disclaimer

One or more of the Following Statements may affect this Document

- This document has been reproduced from the best copy furnished by the organizational source. It is being released in the interest of making available as much information as possible.

- This document may contain data, which exceeds the sheet parameters. It was furnished in this condition by the organizational source and is the best copy available.

- This document may contain tone-on-tone or color graphs, charts and/or pictures, which have been reproduced in black and white.

- This document is paginated as submitted by the original source.

- Portions of this document are not fully legible due to the historical nature of some of the material. However, it is the best reproduction available from the original submission.

9950-931

PROCESS RESEARCH OF POLYCRYSTALLINE SILICON MATERIAL

(PROPSM)

QUARTERLY REPORT NO. 2

JANUARY 1, 1984 THROUGH MARCH 31, 1984

CONTRACT NO. 956698

SOLAREX
Corporation

PROCESS RESEARCH OF POLYCRYSTALLINE SILICON MATERIAL

(PROPSM)

QUARTERLY REPORT NO. 2

JANUARY 1, 1984 THROUGH MARCH 31, 1984

CONTRACT NO. 956698

BY

J. S. CULIK

SOLAREX CORPORATION
1335 PICCARD DRIVE
ROCKVILLE, MD 20850
(301) 948-0202

TABLE OF CONTENTS

I.   INTRODUCTION

This report summarizes work performed during the second quarter of an effort that began in November, 1983. The intent of this program is to develop a passivation process (hydrogenation) that will improve the power generation of solar cells fabricated from presently-produced, large-grain, cast polycrystalline silicon (Semix), a potentially low-cost material. The program will consist of two phases. The first objective will be to verify the operation of a DC plasma hydrogenation system and to investigate the effect of hydrogen on the electrical performance of a variety of polycrystalline silicon solar cells. The second objective will be to parameterize and optimize a hydrogenation process for cast polycrystalline silicon, and will include a process sensitivity analysis.

Section II of this report outlines the sample preparation for the first phase. Section III describes the hydrogenation system; and Section IV summarizes some early results that we have obtained using our hydrogenation system without a plasma. Light-beam induced current (LBIC) measurements of mini-cell samples, and their correlation to dark current-voltage characteristics, are discussed in Section V.

II. PHASE I SAMPLE PREPARATION

The goal of the first phase of this program as described in
the previous report [1] is to determine the fundamental basis
for performance improvements in polycrystalline silicon solar
cells due to the hydrogenation process. Specifically, the
question left unresolved by previous studies is whether hydro-
genation, as it affects the electrical performance of large-
grain cast polycrystalline silicon solar cells, modifies the
bulk or the junction properties of the devices.

As a result of the previous contract, JPL NO. 966902, we
have developed the capability for fabricating and testing small
area photodiodes (so called "mini-cells") on large-area (10cm x
10cm) polycrystalline silicon wafers. We have used this
capability, together with dark current-voltage ("dark I-V")
junction characterization, to analyze the spatial variation of
open-circuit voltage across polycrystalline silicon wafers.

This approach, analyzing small-area photodiodes fabricated
on larger area sample substrates, will be utilized in developing
the hydrogenation process. Wafers with mini-cells will be
fabricated and tested to locate areas where the open-circuit
voltage is substantially degraded. Sample areas of about $4cm^2$
are equivalent to a 5-by-5 matrix of mini-cells. After
characterizing the matrix for dark I-V characteristics and by

2

light-beam induced current (LBIC) measurements to locate elec-
trically-active grain boundaries, the matrix will be hydrogena-
ted and re-analyzed. A comparison of before-hydrogenation and
after-hydrogenation results will indicate the effect of the
process on bulk, junction, and grain boundary recombination.
Selection of the matrix mini-cells will be made so that the
matrix contains both good performance cells (that is, with low
quasi-neutral and space-charge recombination) as well as poor in
order to provide a self-controlled test.

During January a set of mini-cell wafers was fabricated
from a selection of 10cm x 10cm polycrystalline (Semix) wafers.
The wafer set is comprised of sampled wafers from ingots 71-01E,
C4-116B, and C4-108 (which were also utilized in the previous
work, JPL Contract 955902), and wafers from ingots C4-82E and
C4-87E. In addition, several single-crystal wafers were
processed as controls.

The mini-cells wafers were fabricated using the mesa etch
process developed by the previous program [2]. This process
results in an array of up to 400 small (approximately $0.20 cm^2$ in
area) photodiodes ("mini-cells") on 10cm x 10cm wafers. The
diodes are isolated from one another by etching away several
microns of silicon from between the cells, resulting in a mesa
diode structure.

During February, the processing was completed and preliminary testing was begun. The first measurement was shunt conductance because if the shunt conductance is greater than about 1 mmho/cm^2, then the illuminated and dark I-V characteristics will be significantly affected, which will make accurate measurements of them difficult. The results were not encouraging; the shunt conductance was very high and most of the mini-cells from this sample set are virtually unusable. Visual examination of the wafers shows that the mesa isolation is complete. However, selected measurements of open-circuit voltage on "shunted" cells resulted in values below 100 mV. This is indicative of junction faults, and our tentative conclusion is that significant portions of the n$^+$ diffused layer were removed from the active area during the mesa etch.

Because of the problems with these samples, we have begun to fabricate a second set of samples from the same additional wafers. Processing of these samples was halted in early March, however, because the research laboratory at Solarex is being renovated.

III. HYDROGENATION SYSTEM SAMPLE STAGE

Hydrogenation processes are typically performed with the samples in a hydrogen ambient at a temperature that is usually, but not always, above room temperature. Although some hydrogena-

tion processes utilize molecular hydrogen, most require the atomic form, using either an AC or DC plasma or a Kaufman ion source to obtain the ionized species.

For at least the first phase of this program, hydrogenation will be performed using a DC plasma. Some work during the previous quarter was dedicated to modifying a vacuum deposition system for hydrogenation, and locating parts for the substrate heater. A schematic diagram of the substrate stage is show in Figure 1. It consists of a 5cm x 5cm, 0.999 pure, tantalum plate held above the base by ceramic insulators. The plate and sample are heated by a 2.5cm x 2.5cm ceramic heater (Hittman 52800) beneath the plate. The sample temperature is monitored by a type K thermocouple that feeds a temperature controller (Omega 4001KC). A schematic of the temperature control circuit is shown in Figure 2. The heater power is limited by the series resistor to about 20 W. This can be adjusted, as needed. Substrate temperatures up to about 400°C are possible with this design; the low thermal mass of this stage allows the temperature to be ramped up or down very quickly, if necessary.

In operation the chamber is evacuated using mechanical and diffusion pumps, then backfilled with ultra-pure hydrogen. For molecular hydrogen passivation, no voltage will be applied to the top plate. For passivation with ionized hydrogen, a plasma will be obtained by applying a positive voltage in the 300 to

FIGURE 1

6

TYPE K
THERMOCOUPLE

2A

120 VAC

NEUTRAL

OMEGA #4001KC
TEMPERATURE
CONTROLLER

200

30K

NEON

HITTMAN #528000
CERAMIC HEATER
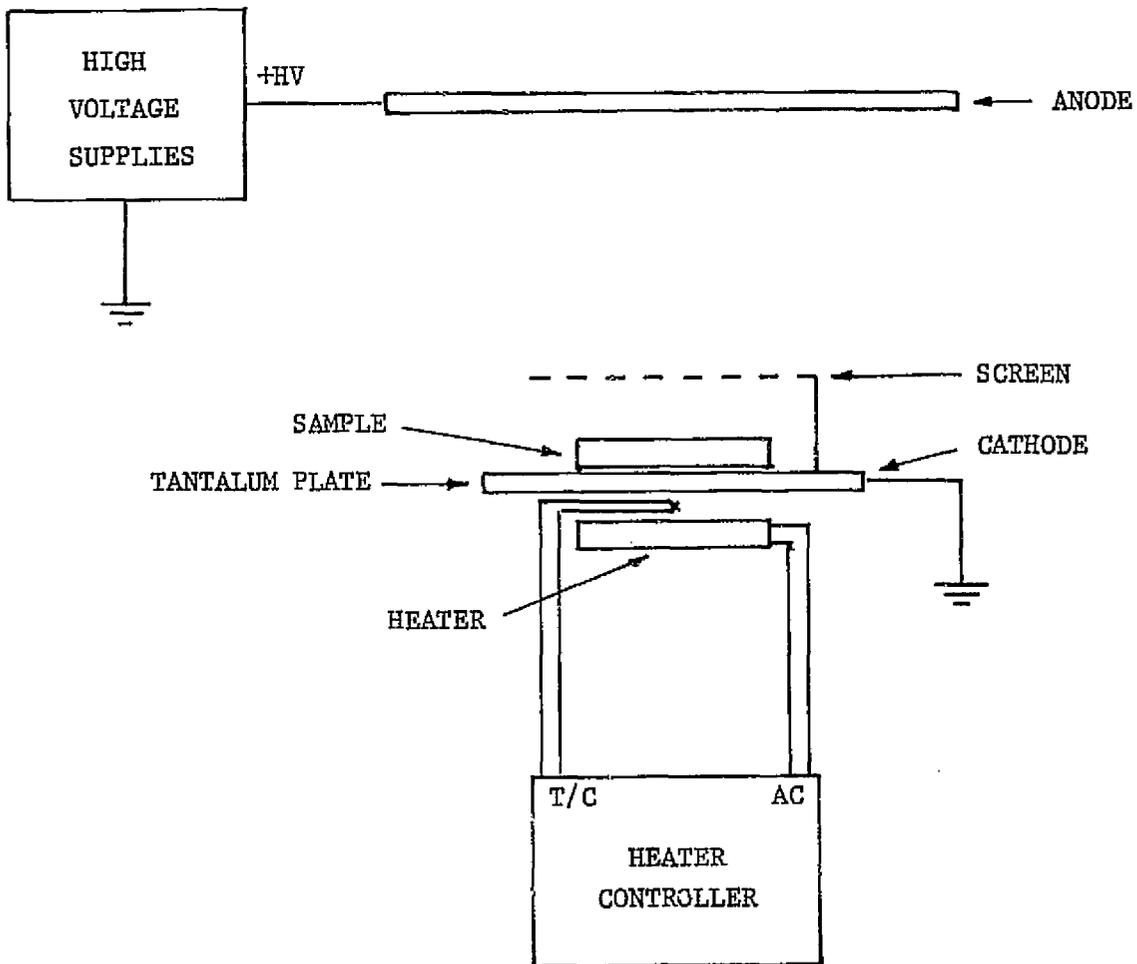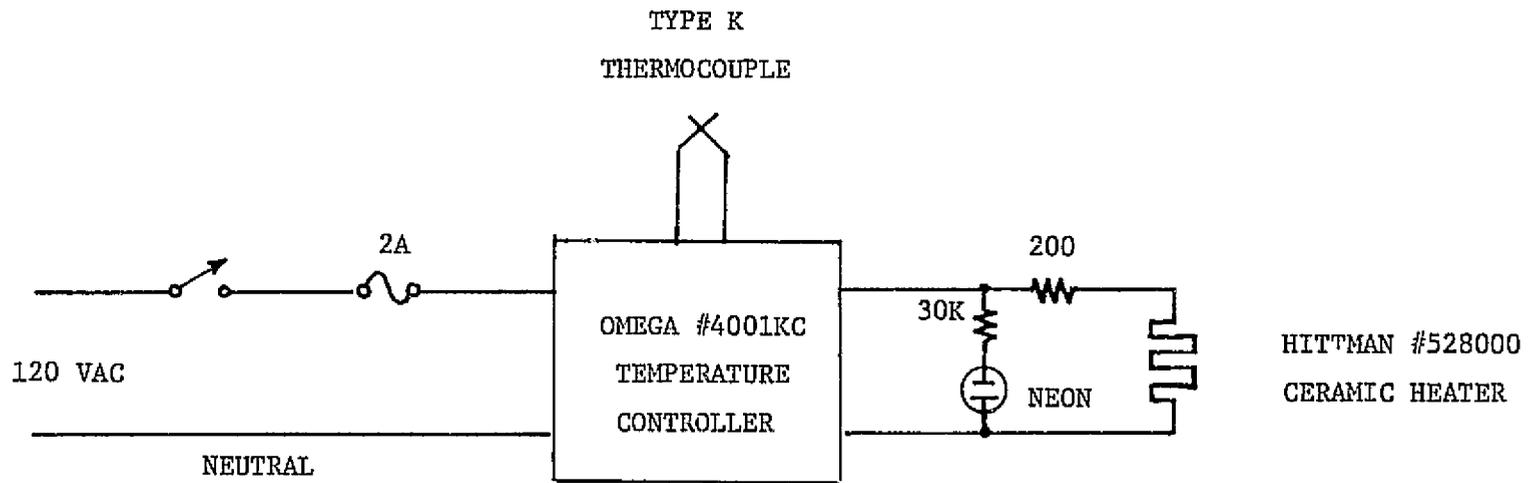
FIGURE 2

1000 volt range to the top plate (anode). The cathode and screen are both held at ground potential.

Two power supplies are available for obtaining the high voltage. The first (HP Model 712B) is useful for lower voltage, higher current (500 V, 200 mA). The other (Kepko Model 1220C) will achieve a higher voltge (1500 V) but with a sacrifice of current (50 mA). Assuming a $25cm^2$ current cross-section, we may be able to obtain maximum current densities of $2mA/cm^2$ (at 1500 V) to $8mA/cm^2$ (at 500 V). We will use both power supplies in order to cover the range of possible accelerating voltages.

IV. MOLECULAR HYDROGENATION

The previous discussion of hydrogenation [1] dealt solely with passivation of polycrystalline silicon by an ionized form of hydrogen, which was obtained by either an AC or DC plasma or by a Kaufman ion source. Some of the research groups that did this work also investigated the use of molecular hydrogen, but found that it apparently does not result in grain boundary passivation. As early as 1979, Seager and Ginley [3] experimented with a number of passivants, including molecular hydrogen, and concluded that molecular hydrogen did not diffuse into the silicon. In 1980, Benton, et.al. [4], passivated defects in laser recrystallized silicon with a 0.38 Torr AC hydrogen plasma at 200°C for 4 hours. They were, however,

unable to effect any measurable defect passivation with a 4 hour anneal in molecular hydrogen.

In contrast, del Valle, et.al. [5], reported on an increase in the minority-carrier diffusion length of Wacker polycrystalline silicon by annealing in molecular hydrogen at 700°C for one hour. Since there was no improvement after a 700°C anneal in nitrogen, they concluded that the change was due to incorporation of hydrogen. However, Benton's group was able to anneal point defects in their laser-recrystallized silicon by a thermal anneal at 700°C [6], and this thermally-related defect anneal may invalidate del Valle's claim of molecular hydrogen passivation.

To further clarify this difference between atomic and molecular hydrogenation, Johnson, et.al. [7], investigated hydrogen passivation of grain boundaries of silicon deposited by low pressure chemical vapor deposition (LPCVD) using deuterium, in order to be able to detect its presence by using SIMS. They found that monatomic deuterium at 350°C permeated the film, whereas the concentration of molecular deuterium after a 400°C anneal for one hour was negligible. These particular results indicate that little, if any, molecular hydrogen was retained by the grain boundaries.

However, several other groups have recently reported that molecular hydrogen is in fact useful for improving polycrystalline silicon. In 1982, Lam [8] reported on reducing the sheet resistance (or increasing the conductance) of LPCVD polycrystalline by annealing in molecular hydrogen at 450°C for 30 minutes. After heating to 600°C, the sheet resistance had returned to its pre-anneal value, indicating that the change was due to incorporation of hydrogen in the film.

Amzil, et.al. [9], recently reported that they were able to obtain improvements in the effective minority-carrier diffusion length of Wacker and CGE polycrystalline silicon by both molecular and atomic hydrogen. The increase due to annealing in molecular hydrogen at 300°C for times longer than two hours was similar to, but not as large as, that obtained by AC plasma and Kaufman ion source hydrogenation. Anneals in argon at similar temperature and time had no effect. These results are interesting but not conclusive since there were no solar cell results (such as short-circuit current, open-circuit voltage, and fill-factor) reported.

During this quarter, we began an experiment to investigate the usefulness of molecular hydrogen annealing on polycrystalline solar cells. Several samples were selected from 4cm^2 solar cells fabricated for the thickness-resistivity matrix of the previous program (JPL Contract No. 955902). The cells were

fabricated from 1.5 ohm-cm polycrystalline silicon wafers supplied by Semix, Inc., chemical-polish etched to a thickness of 250 microns, diffused to 70 ohms/square, and alloyed with Englehard A-3484 aluminum paste to compensate the back junction. The metallization system was evaporated Ti-Pd with electroplated Ag. The front contacts were a standard Solarex fine-line chevron pattern, which was photolighographically-defined. The wafers were sintered for 15 seconds at about 475°C before being sawn into 4cm^2 cells, and were sintered an additional 15 seconds after a tantalum oxide anti-reflection (AR) coating was electron-beam evaporated. For this hydrogen annealing experiment, the AR-coating was removed by an HF-vapor etch.

The particular cells for molecular hydrogen annealing were chosen using two criteria: (1) low open-circuit voltage; and (2) low shunt conductance. Cells that meet these conditions must have an open-circuit voltage loss mechanism that is <u>not</u> related to a simple ohmic shunt, that is, probably not due to process-induced faults. Non-shunted cells with low open-circuit voltage are more likely to have a material-related loss mechanism. As discussed in the following section, a cell which contains a large number of electrically-active grain and sub-grain boundaries will have values of open-circuit voltage that are significantly degraded. The first cell that was annealed (cell 1-8) had an open-circuit voltage of 537mV (at 135 mW/cm^2, 25°C) and a shunt conductance of about 0.07 mmho/cm^2. This non-

11

AR-coated cell also had a light-generated current density of 22.7 mA/cm^2 at 135 mW/cm^2 incident power. For comparison, a single-crystal cell typically has a light-generated current density of 27 to 28 mA/cm^2. Illuminated and dark I-V characteristics were measured, and the cell was annealed in high purity hydrogen at 1 Torr and 300°C for one hour. The illuminated and dark I-V characteristics were again measured, and the cell was then returned to the hydrogenation system. Measurements were made after 1, 2, 5, 10 and 20 (total) hours. Figure 3 shows the dark I-V curve before annealing and after 10 hours. There is no improvement in the dark characteristics. In fact, the space-charge component appears to have increased slightly. The open-circuit voltage change was within the measurement uncertainty. Therefore, we conclude that basically no change has occurred as a result of molecular hydrogen passivation.

It may be, however, that this cell has a low value of open-circuit voltage due to a short minority-carrier diffusion length that is not related to electrically-active grain or sub-grain boundaries. This problem is suggested by the value of light-generated current that is considerably lower (by about 15%) than that of single-crystal cells. Therefore, we will continue this experiment by choosing several additional cells for molecular hydrogenation under the following new criteria: (1) low open-circuit voltage; (2) low shunt conductance; and (3) high light-generated current. This will hopefully insure that the open-

12

FIGURE 3

MOLECULAR HYDROGEN ANNEAL

1 Torr, 300°C

CELL 1-8

AFTER 10 HOURS

BEFORE ANNEAL

CURRENT DENSITY (mA/cm²)

VOLTAGE (mV)

13
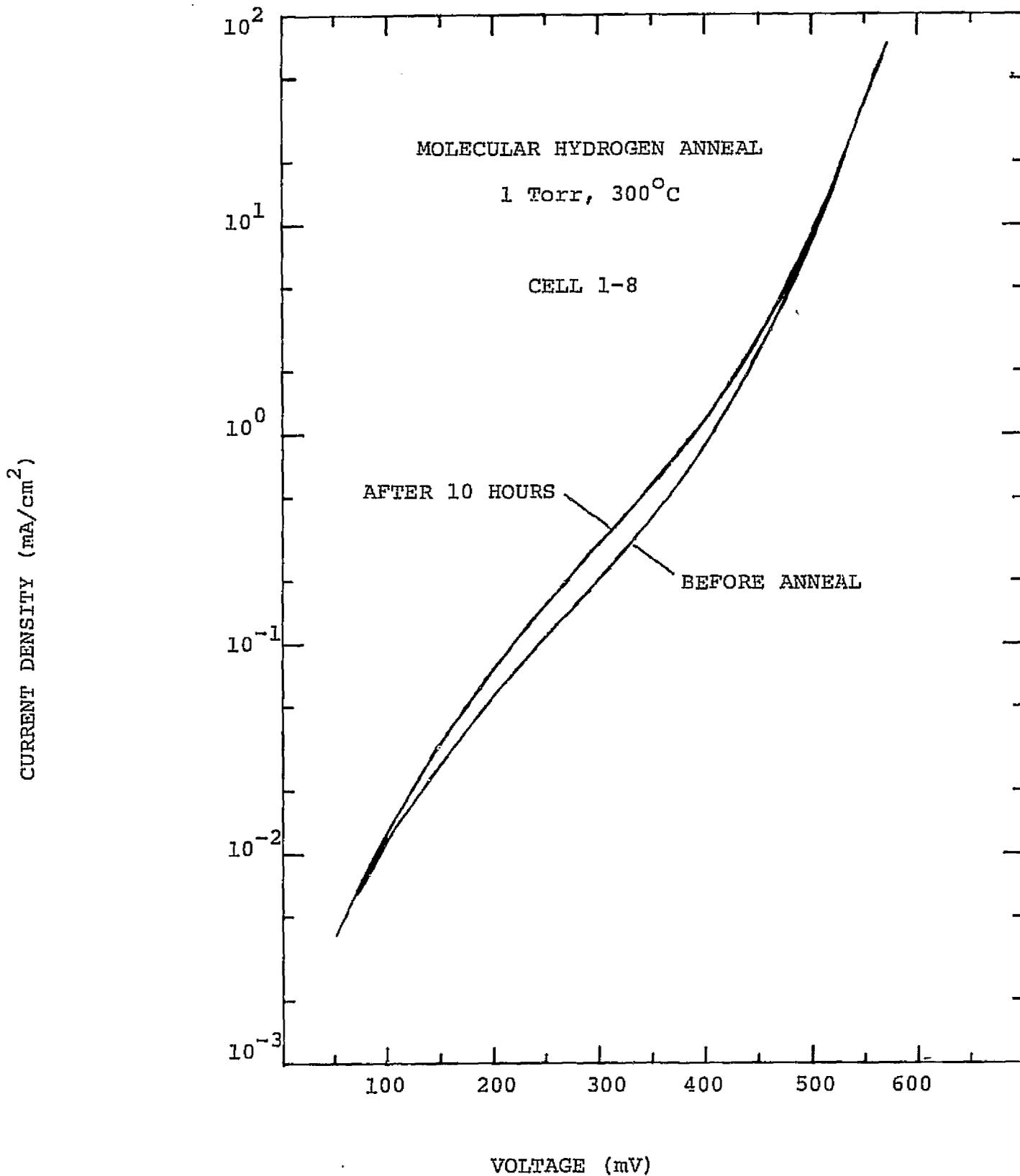
circuit voltage is degraded solely by grain boundary-related defects.

V. LIGHT-BEAM INDUCED CURRENT (LBIC)

Electron-beam induced current (EBIC) and light-beam induced current (LBIC) measurements are techniques that are commonly used to locate and image electrically-active defects in devices. The two techniques are complementary in that EBIC has much finer resolution (less than 10 microns), but very shallow penetration, while LBIC, though not as fine in resolution (much greater than 10 microns), allows one to choose the penetration depth by varying the wavelength of the light. Thus, both surface and bulk defects, if large, can be imaged with LBIC by choosing the correct wavelength.

Results from the previous contract (JPL Contract No. 955902) indicated that much of the open-circuit voltage loss in large-grain polycrystalline solar cells was due to excess quasi-neutral (bulk) recombination. Thus, significant improvements to the performance of these cells will occur only if bulk recombination processes are reduced. Techniques to evaluate bulk recombination processes, specifically dark I-V characteristics and long-wavelength LBIC, will be used in this program to study the effect of hydrogen passivation on polycrystalline silicon solar cell performance.

Solarex has had LBIC capabilities for several years. However, the system was originally designed for 4cm^2 solar cells. During this quarter, the LBIC system was modified to accomodate mini-cell wafers. This was accomplished by adding a magnetic probe and a steel baseplate to the existing sample stage. No changes to the system software were required. However, a considerable amount of effort was needed to eliminate noise sources in the system and to determine the system parameters for use with mini-cells.

LBIC system capability was demonstrated by scanning selected areas of two mini-cell wafers used in the previous program (JPL Contract 955902). Measurements were made at an LBIC wavelength of 800 nm; the light penetration depth into the silicon is about 10 microns at this wavelength. Figures 4 and 5 show two LBIC scans from regions of mini-cell wafer C4-116B. In Figure 4 (mini-cells 12-7, 12,8, 13-7, 13-8), there is a strong correlation between electrically-active grain-boundary content, open-circuit voltage, and quasi-neutral recombination. Cell 13-7 has very little grain-boundary activity and the lowest value of J_{QNO}. The inset shows a photograph of an area to the left; there are many twin boundaries in cell 13-7. But they are not electrically-active and do not cause the quasi-neutral recombination current to increase. In contrast, cells 13-8 and 12-8 have progressively more LBIC-imaged grain-boundary activity, greater quasi-neutral and space-charge recombination,

15

FIGURE 4

12-7

12-8

506 mV, 31.0 mA/cm^2 34.9 x 10^{-9} mA/cm^2 530 mV, 30.3 mA/cm^2 26.2 x 10^{-9} mA/cm^2

(65%)   1.7 x 10^{-2} mA/cm^2 (2.9)   (64%)   1.4 x 10^{-2} mA/cm^2 (3.2)

13-7

13-8

571 mV, 31.9 mA/cm^2 5.0 x 10^{-9} mA/cm^2 540 mV, 31.0 mA/cm^2 12.7 x 10^{-9} mA/cm^2

(64%)   5.9 x 10^{-4} mA/cm^2 (2.2)   (52%)   2.0 x 10^{-3} mA/cm^2 (2.3)

KEY

V_{oc}, J_{sc} J_{QNO}

(FF) J_{SCO} (n-factor)

16
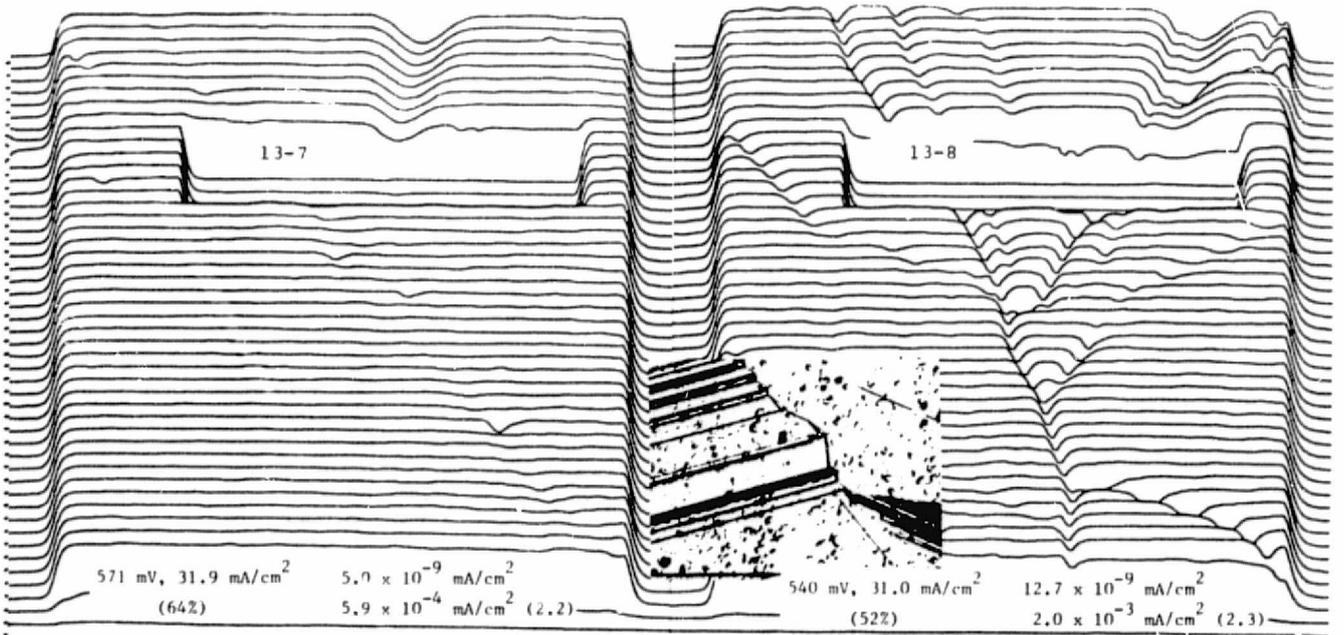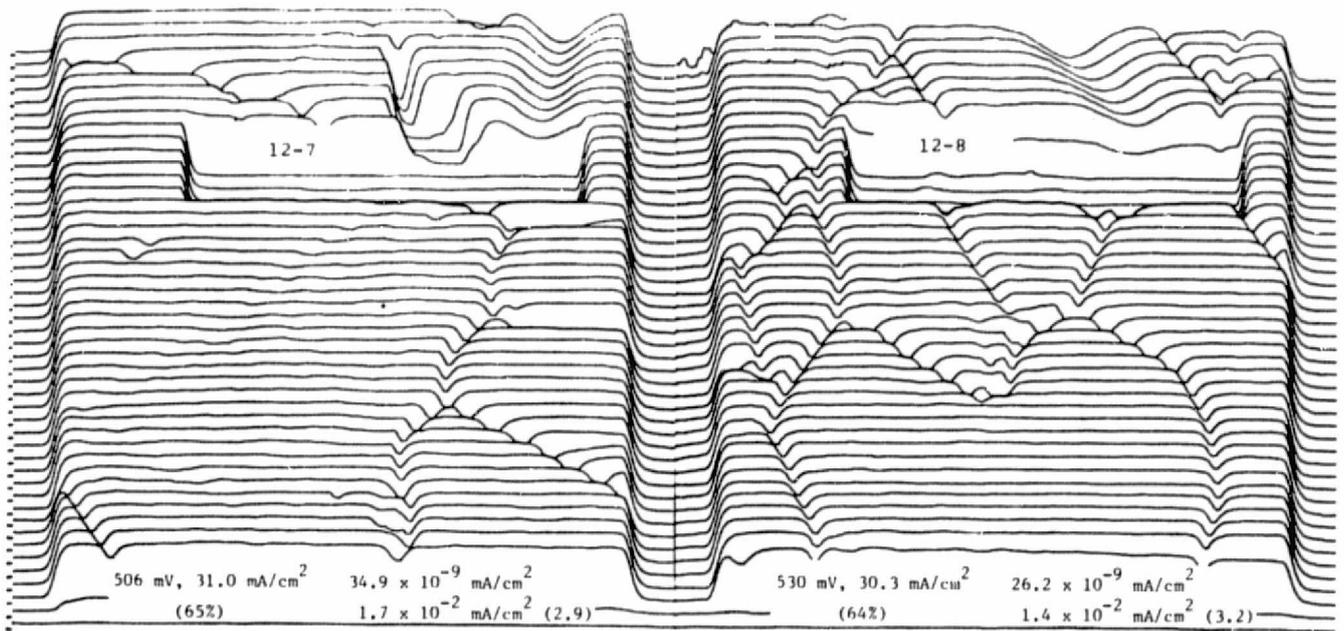
lower open-circuit voltage, and lower light-generated current density. Cell 12-7 has the lowest open-circuit voltage and the greatest amount of quasi-neutral recombination, but less LBIC-imaged grain-boundary activity.

Similar correlation between grain-boundary activity and quasi-neutral recombination is shown in Figure 5 (mini-cell wafer C4-116B; cells 13-2, 13-3, 14-2, 14-3). Cell 13-2, which has the least amount of LBIC-imaged grain-boundary recombination, also has the lowest bulk recombination and the highest open-circuit voltage. Next to it, cells 13-3 and 14-2 have considerably more grain-boundary activity, lower open-circuit voltage, significantly greater quasi-neutral recombination, but space-charge recombination that is only slightly greater than cell 13-2. Cell 14-3 has an extremely large value of space-charge recombination but much less grain-boundry activity than cells 13-3 or 14-2. These results would seem to indicate that space-charge recombination is not correlated with grain-boundary recombination. Also, the fill-factor does not appear to suffer due to grain-boundary recombination (compare cells 13-2 and 14-2).

Figure 6 and 7 show LBIC scans from two regions of mini-cell wafer 71-01E/TOP that have a large number of subgrain (small-angle) boundaries. These scans were also made at an LBIC wavelength of 800 nm. Figure 6 (cells 3-4, 4-4, 3-3, and 4-3)

17

13-2

1 mm

579 mV, 31.0 mA/cm^2 4.9 x 10^{-9} mA/cm^2
(66%)   9.2 x 10^{-5} mA/cm^2 (2.1)

13-3

563 mV, 29.7 mA/cm^2 8.8 x 10^{-9} mA/cm^2
(65%)   7.0 x 10^{-5} mA/cm^2 (2.1)

14-2

568 mV, 30.1 mA/cm^2 7.2 x 10^{-9} mA/cm^2
(66%)   9.3 x 10^{-5} mA/cm^2 (2.0)

14-3

556 mV, 30.5 mA/cm^2 8.4 x 10^{-9} mA/cm^2
(60%)   1.2 x 10^{-1} mA/cm^2 (4.7)

FIGURE 5

18
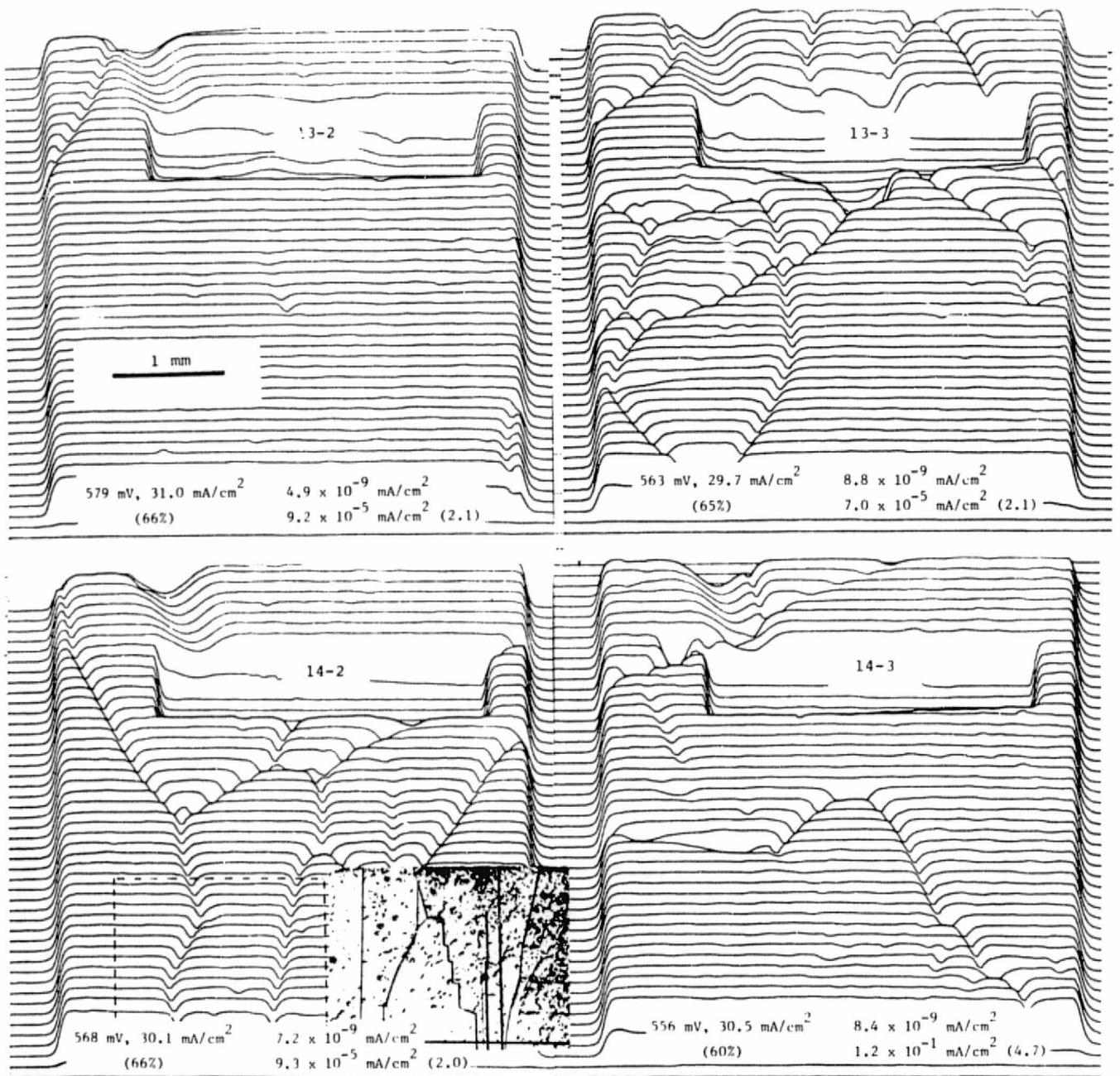
once again shows a very strong correlation between LBIC-imaged grain-boundary activity and quasi-neutral recombination. The insets are of an area to the right which has a considerable amount of LBIC-activity. The right inset shows that there are not many grain boundaries in this area. However, the left inset, of a defect-etched serial wafer, shows that there are many dislocations in this region which form subgrain boundaries that act to reduce the electrical grain size. Quasi-neutral recombination increases progressively from cell 3-3, to 3-4, 4-4, and 4-3 by a factor of two. The open-circuit voltage decreases by 21 mV. The fill-factor of all of these cells is not significantly different. However, the space-charge recombination of cell 4-3, with the greatest number of electrically-active grain boundaries, is significantly less than that of cell 3-3, which has the least amount of LBIC-imaged grain boundary activity.

Figure 7 (mini-cell wafer 71-01E/TOP; cells 4-17, 4-16, 3-17, and 3-16) shows another area that has a large number of subgrain boundaries. The effect of these boundaries is to significantly increase the bulk recombination (by a factor of three in this case; compare cell 4-17 to 4-16). Several small areas of localized subgrain boundaries apparently degrade the cell more than one larger area, as shown by comparing cells 3-16 and 3-17. Space-charge recombination is not significantly affected by subgrain-boundary recombination. The fill-factors of these cells are not significantly different.

19

FIGURE 6

1 mm

4-17

4-16

544 mV, 26.3 mA/cm²   14.0 x 10⁻⁹ mA/cm²
(72%)   4.2 x 10⁻⁵ mA/cm² (1.8)

576 mV, 28.3 mA/cm²   4.8 x 10⁻⁹ mA/cm²
(70%)   4.3 x 10⁻⁴ mA/cm² (2.4)

3-17

3-16

567 mV, 26.8 mA/cm²   5.2 x 10⁻⁹ mA/cm²
(68%)   1.4 x 10⁻⁴ mA/cm² (2.0)

560 mV, 27.1 mA/cm²   8.9 x 10⁻⁹ mA/cm²
(70%)   6.4 x 10⁻⁴ mA/cm² (2.4)

FIGURE 7

21
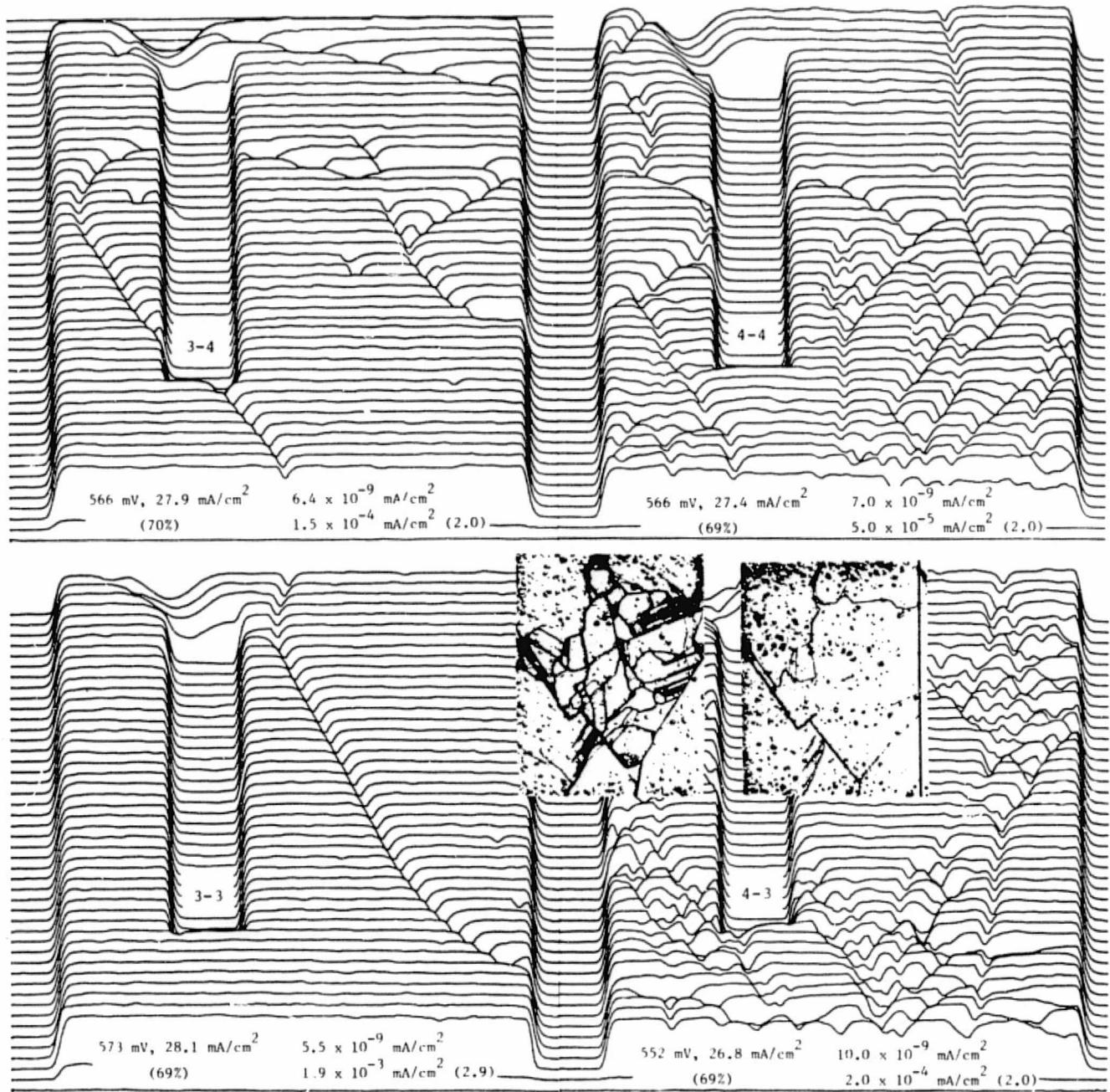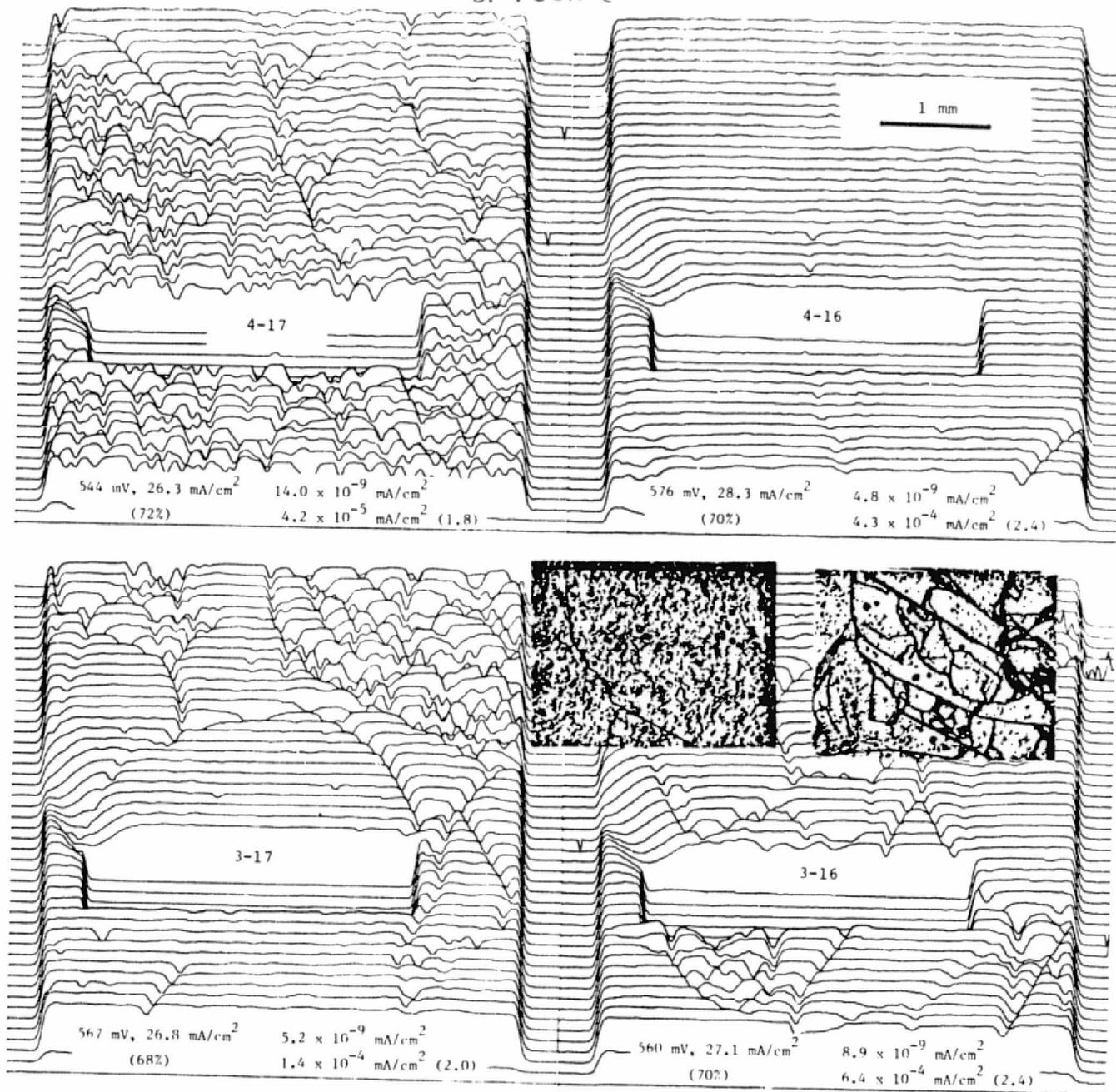
In summary, electrically-active grain and subgrain boundaries severely impact the bulk recombination of large-grain, cast polycrystalline silicon solar cells. In most cases, no change is observed in space-charge recombination; however, there does appear to be an additional "defect" that causes the space-charge recombination to increase by several orders of magnitude. This defect appears to be localized to areas smaller than one mini-cell (about 0.2 cm^2) and is not resolved by LBIC.

VI. PLANS

Work during the next quarter (April to June, 1984) will be limited due to the renovation of the Solarex research laboratory. When the laboratory is operational, work will commence on the Phase I sample set and it should be completed by the end of the quarter. Several additional cells will be annealed in hydrogen to investigate any effects of molecular hydrogen on performance. We will also begin some preliminary hydrogen plasma experiments to correct any problems with the DC plasma system.

ACKNOWLEDGEMENTS

The molecular hydrogenation experiments were performed by K. Grimes who also prepared the LBIC samples. The author would like to thank S. Johnson for helpful comments, and to acknowledge the assistance of P. Fazio in the preparation of this report.

22

REFERENCES

1. J. Culik, "Process Research of Polycrystalline Silicon Material (PROPSM)", JPL Contract No. 956698, First Quarterly Technical Report, 1984.

2. J. Culik, "Process Research on Polycrystalline Silicon Material (PROPSM)", JPL Contract No. 955902, Final Technical Report, 1984.

3. C.H. Seager and D.S. Ginley, "Passivation of Grain Boundaries, in Polycrystalline Silicon", Appl. Phys. Lett., 34, 337 (1979).

4. J.L. Benton, C.J. Doherty, S.D. Ferris, D.L. Flamm, L.C. Kimerling, and H.J. Leamy, "Hydrogen Passivation of Point Defects in Silicon", Appl. Phys. Lett., 36, 670 (1980).

5. J.L. del Valle, C. Flores, and F. Duenas, "Hydrogenation Effects in Cast Polycrystalline Silicon p-n Junction Solar Cells", 14th IEEE Photovoltaic Specialists Conf. (1980), 202.

6. J.L. Benton, C.J. Doherty, L.C. Kimerling, H.J. Leamy, D.L. Flamm, and S.D. Ferris, in "Laser and Electron Beam Processing of Materials", (Materials Research Society, Boston, 1979).

7. N.J. Johnson, D.K. Biegelsen, and M.D. Moyer, "Deuterium Passivation of Grain-Boundary Dangling Bonds in Silicon Thin Films", Appl. Phys. Lett., 40, 822 (1982).

8. H.W. Lam, "Conductivity Enhancement in Laser-Recrystallized Polycrystalline-on-Insulator using Molecular Hydrogen Annealing", Appl. Phys. Lett., 40, 54 (1982).

9. H. Amzil, M. Sebbar, G. Athian, L. Ammar, and S. Martinuzzi, "Influence of Annealing in Atomic and Molecular Hydrogen on Diffusion Lengths of p-type Polysilicon", 5th E. C. Photovoltaic Solar Energy Conf., 1983.

WORK ELEMENT	1	2	3	4	5	6	7	8	9	10	11	12
PROGRAM SCHEDULE — MONTH												
HYDROGENATION												
1. FUNDAMENTAL MECHANISMS		████	████	████	████	───	───					
2. PROCESS DEVELOPMENT						═══	═══	═══	═══	═══		
3. PROCESS CONTROL/SENSITIVITY										▽		
4. PROCESS COST ANALYSIS											▽	
PROGRAM MANAGEMENT												
1. PROGRAM PLAN	▼											
2. MONTHLY TECHNICAL REPORT		▼		▼	▼		▽	▽		▽	▽	
3. QUARTERLY TECHNICAL REPORT			▼			▼			▽			
4. DRAFT FINAL TECHNICAL REPORT												▽
5. FINAL TECHNICAL REPORT												(▽)
6. MONTHLY FINANCIAL REPORT		▼	▼	▼	▼	▽	▽	▽	▽	▽	▽	▽ (▽)
7. PIM					▼						▽	
8. BIMONTHLY SHIPMENT		▽		▽		▽		▽		▽		